MAE 263F Midterm Report: Snake Project

Sarah Enayati and Jonathan Gray

I. INTRODUCTION

This project attempts to design a robotic snake that mirrors the movements of biological snakes to navigate through and operate within challenging environments with various Reynolds numbers that typically are inaccessible to traditional UAVs. We attempt to construct an analytical framework that accurately represents the snake-like undulation and its interactions with viscous fluids. This framework will allow the robotic snake to optimize movement and control in ways that traditional UAVs cannot, thus achieving longer mission durations and requiring less energy.

II. METHODOLOGY

In this project, we model the locomotion of a snake using a discretized representation of a rod, using resistive force theory (RFT) approach to estimate the resistive forces, specifically viscous force, acting on the snake due to its interaction with the surrounding medium. We also use slender body theory (SBT) to model the hydrodynamic forces. SBT is appropriate for analyzing slender, elongated bodies moving in a fluid, as it provides a more accurate representation of the viscous forces acting on the body as the body moves through and interacts with the fluid. By applying SBT, we calculate the drag coefficients that resist motion both along and perpendicular to the rod's axis, using the methodology described in Appendix A. This allows us to simulate the impact of hydrodynamic influences, including the interactions between adjacent segments of the rod.

Our internal forces for our simulation are composed of bending and stretching resistances, and our external forces is viscous damping due to the surrounding environment. To implement these forces, we use the Newton-Raphson method, solving for node displacements at each time step based on the balance of forces. We simplify the Jacobian matrix to reduce computational complexity by approximating/neglecting terms whose effects can be thought of as minimal.

To simulate the snake's undulatory motion, sinusoidal transverse motion is applied to the head of the rod. The head motion is defined by the function:

$$y_{head} = A * \sin(\omega * t) \tag{1}$$

where A is the amplitude and ω is the frequency. The rest of the body evolves dynamically. The tail end of the rod, on the other hand, is free to move, allowing full propagation of waves generated at the head throughout the entire body length. The head's velocity, the derivative of the sinusoidal function above, is applied as a boundary condition for the first node. These boundary conditions are chosen to mimic biological snakes, where head movements control the body, providing the necessary undulatory motion for propulsion.

Please see Appendix A for Algorithm 1.

III. PRELIMINARY RESULTS: SENSITIVITY ANALYSIS FOR PARAMETER DETERMINATION

In our sensitivity analysis, we use the average x-direction velocity as our performance metric to evaluate the effects of different parameters (number of nodes, length of snake, and hydrodynamic influence range) on the locomotion efficiency of the robotic snake. The x-direction velocity represents the snake's forward speed, which indicates how well it can propel itself through a fluid environment using undulation.

A. Nodal Determination

We vary the number of nodes in the robotic snake to understand its effect on locomotion efficiency and average velocity and thus determine the optimal number of nodes for our snake. The number of nodes determines how well the wave propagates along the body, directly impacting the smoothness of movement and overall propulsion. As we increase the number of nodes from 5 to 18, we observe a significant improvement in average velocity [see Figure 1.] A higher number of nodes allows for smoother and more continuous undulatory movement, which generates more effective thrust. However, beyond 16 nodes, the velocity begins to plateau, with only minimal increases up to 18 nodes. This plateau suggests that additional nodes do not significantly enhance propulsion but instead add computational complexity and potentially increase drag resistance. Based on these results, we choose the optimal number of nodes to be 16. This balances achieving high velocity and minimizing unnecessary computational load, and ensures efficient movement without overcomplicating the model or reducing performance due to added drag.

B. Snake Length

We also conducted sensitivity analysis on the total length of the robotic snake to understand its influence on locomotion efficiency and average velocity. The length of the snake is a critical parameter because it affects both the wave propagation dynamics and the drag experienced by the body as it moves through the fluid. A longer snake generally allows for more undulation cycles along its body, which can generate greater propulsion due to more efficient transmission of waves. However, this increased length also results in more surface area interacting with the fluid, therefore increasing drag resistance. The longer the snake, the greater the cumulative drag that each segment must overcome, which can result in decreased average velocity. On the other hand, a shorter snake experiences less

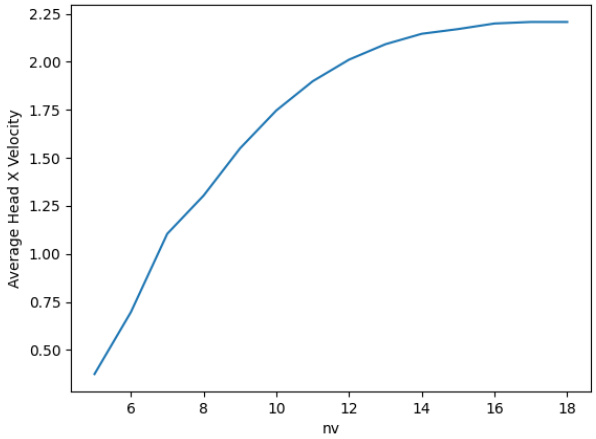

Fig. 1. Sensitivity Analysis on Number of Nodes

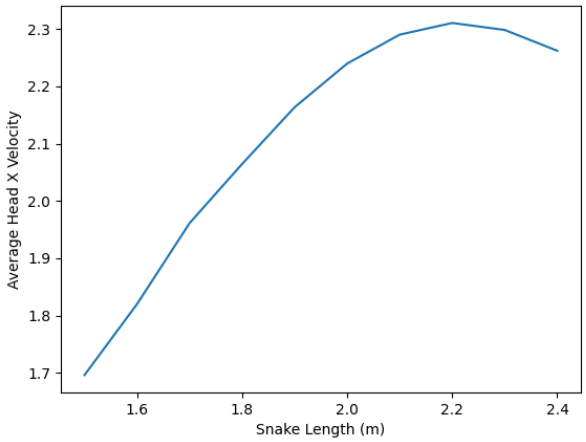

Fig. 2. Sensitivity Analysis on Snake Length

overall drag, which may increase velocity, but it may also lack the sufficient wave propagation length needed to generate effective thrust. This would lead to reduced propulsion efficiency. By analyzing different snake lengths, we evaluated the trade-off between propulsion generation and fluid resistance, which allowed us to identify an optimal length that maximizes velocity while maintaining stability.

In our sensitivity analysis of the robotic snake's total length, we vary the rod length from 1.5 to 2.4 meters and observe its effect on the average velocity, as can be seen in Figure 2.

These results indicate that as the snake length increases, the average velocity initially improves, but starts declining again after reaching a peak of 2.2 meters. This is due to the increase in drag resistance as the length increases further, ultimately reaching a point where the additional surface area interacting with the fluid negates the propulsion gains. Based on these results, a snake length of 2.2 meters is optimal, as it maximizes average velocity without introducing significant drag penalties.

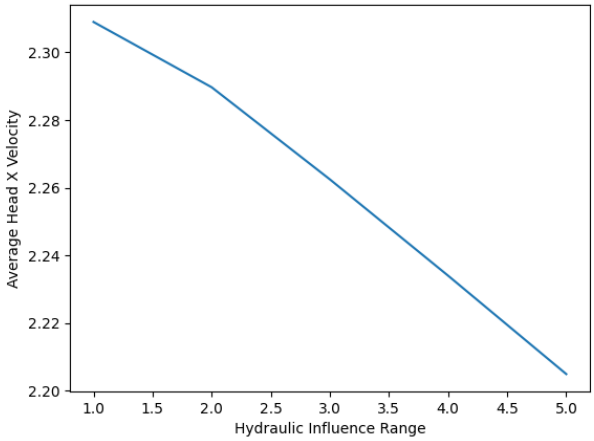

Fig. 3. Sensitivity Analysis on hydraulic influence range, using a range of 1, 2, 3, 4, 5

C. Hydrodynamic Influence Range

The hydrodynamic influence range refers to the number of neighboring segments that are considered to interact with a given segment in the fluid environment. A higher hydrodynamic influence range results in a more accurate simulation of fluid interactions, as more neighbors are taken into account when calculating the forces. This means that the model can better represent how segments affect one another through the surrounding fluid, similar to real-world behavior in water. However, increasing the hydrodynamic influence range also increases computational complexity. Each segment interacts with more neighbors, requiring more calculations and thus greater computational resources. Thus, we want to choose a sufficiently high enough value to be accurate yet computationally efficient.

We vary our hydrodynamic influence range between 1 to 5 and record the average velocity. We keep all other parameters the same as seen in Figure 3.

As you can see from the plot above, the average velocity is consistently decreasing. This is because increasing the hydrodynamic influence range introduces more drag or more interaction effects between the segments, resulting in lower propulsion efficiency.

To balance model accuracy and efficiency, we choose to select a hydrodynamic influence range of 3. This choice ensures that important fluid interactions are captured while avoiding the excessive computational cost and diminished velocities associated with larger ranges.

IV. Appendix A

Algorithm 1 Get Hydrodynamic Force (getFh)

Input: $q_{new}, q_{old}, C_t, C_n, range, nv$
Output: F_{hydro}, J_{hydro}
for each node, k, in snake body: **do**
  // tangents and normals are calculated
  $\hat{t} = \frac{q_{k+1}-q_k}{|q_{k+1}-q_k|}$
  $\hat{n} = [-\hat{t}[1], \hat{t}[0]]$
  // tangential and normal velocity and forces are calculated
  $v_t = u_k \cdot \hat{t}$
  $v_n = u_k \cdot \hat{n}$
  $F_t = -C_t * v_t$
  $F_n = -C_n * v_n$
  // Hydrodynamic force is updated for all DOF
  $F_{hydro} = F_{hydro} + F_t + F_n$
  // Hydrodynamic Jacobian is updated for all DOF
  $J_t = \frac{-C_t}{dt} * \hat{t} \otimes \hat{t}$
  $J_n = \frac{-C_n}{dt} * \hat{n} \otimes \hat{n}$
  $J_{hydro} = J_{hydro} + J_t + J_n$
  for each node, j, in range: do
    $F_{interaction} = \frac{(C_n(u_j-u_k)\cdot\hat{r})*\hat{r}+C_t((u_j-u_k)-(u_j-u_k)\cdot\hat{r}*\hat{r})}{|r|}$
    $F_{hydro}[k] = F_{hydro}[k] + F_{interaction}$
    $F_{hydro}[j] = F_{hydro}[j] - F_{interaction}$
    $J_{interaction} = \frac{C_n*\hat{r}\otimes\hat{r}+C_t*(I-\hat{r}\otimes\hat{r})}{|r|}$
    // Update Jacobian
    $J_{hydro}[k,k] = J_{hydro}[k,k] + J_{interaction}$
    $J_{hydro}[k,j] = J_{hydro}[k,j] - J_{interaction}$
    $J_{hydro}[j,j] = J_{hydro}[k,k] - J_{interaction}$
    $J_{hydro}[j,j] = J_{hydro}[j,j] + J_{interaction}$
  end for
end for
Return F_{hydro}, J_{hydro}

Algorithm 2 Snake Locomotion Simulation

Input: tol
Output: ...
$err \leftarrow \infty$
while $err > tol$ **do**
  // Stretching and bending forces calculated from predefined functions
  // Calculate viscous force and its Jacobian (using RFT)
  $F_V = -C(q_{new} - q_{old})/dt$
  $J_V = -C/dt$
  // Calculate hydrodynamic force and hydrodynamic interaction forces (getFh)
  $F_{hydro} = getFh(q_{new}, q_{old}, C_t, C_n, nv)$
  // Calculate Equation of Motion
  $f = M * \frac{q_{new}-q_{old}}{\Delta t^2} - M * \frac{u_{old}}{\Delta t^2} - (F_b + F_s + F_v + F_{hydro})$
end while

References

[1] A. Yamano, K. Shimizu, M. Chiba, H. Ijima, Fluid force identification acting on snake-like robots swimming in viscous fluids, Journal of Fluids and Structures, Volume 106, 2021, 103351, ISSN 0889-9746, https://doi.org/10.1016/j.jfluidstructs.2021.103351

[2] A. Yamano, T. Kimoto, Y. Inoue, M. Chiba, Optimal swimming locomotion of snake-like robot in viscous fluids, Journal of Fluids and Structures, Volume 123, 2023, 104007, ISSN 0889-9746, https://doi.org/10.1016/j.jfluidstructs.2023.104007.

[3] Moore, B. R. (n.d.). Snake locomotion. University of Louisiana at Lafayette. Retrieved October 30, 2024, from https://userweb.ucs.louisiana.edu/~brm2286/locomotn.htm

[4] Cicconofri, G., & DeSimone, A. (2015). A study of snake-like locomotion through the analysis of a flexible robot model. *Proceedings of the Royal Society A: Mathematical, Physical and Engineering Sciences, 471*(2182), 20150054. https://doi.org/10.1098/rspa.2015.0054

[5] Kimoto, T., Yamano, A., & Chiba, M. (2023). Estimation of fluid forces on a snake-like robot swimming in viscous fluids considering boundary layer thinning. In *2023 IEEE/SICE International Symposium on System Integration (SII)* (pp. 1-6). IEEE. https://doi.org/10.1109/SII55687.2023.10039336

[6] G. Taylor, "Analysis of the Swimming of Long and Narrow Animals," *Proceedings of the Royal Society of London. Series A, Mathematical and Physical Sciences*, vol. 214, no. 1117, pp. 158-183, Feb. 1952.

[7] Païdoussis, Michael P., Stuart J. Price, and Emmanuel De Langre. Fluid-structure interactions: cross-flow-induced instabilities. Cambridge University Press, 2010

[8] Jawed, M. Khalid, Alyssa Novelia, and Oliver M. O'Reilly. *A primer on the kinematics of discrete elastic rods*. Berlin/Heidelberg, Germany: Springer International Publishing, 2018.

[9] Gray, James. "The mechanism of locomotion in snakes." Journal of experimental biology 23.2 (1946): 101-120.